

Static and dynamic models for the electric environmental control system in initial design

Marco Fioriti¹

Department of Mechanical and Aerospace Engineering, Politecnico di Torino, C.so Duca degli Abruzzi n.24, Turin, Italy

Guido Pavan²

Department of Mechanical and Aerospace Engineering, Politecnico di Torino, C.so Duca degli Abruzzi n.24, Turin, Italy

Sofia Caggese³

Department of Mechanical and Aerospace Engineering, Politecnico di Torino, C.so Duca degli Abruzzi n.24, Turin, Italy

The environmental control is the system that requires the most power of all the aircraft on-board systems. Considering the need to reduce fuel burnt and the consequent pollutions, a way to improve its efficiency is to electrify that system enabling the bleedless engine technology. This paper describes the activities carried out to size the electric environmental control system and to model its dynamic behaviors. The thermodynamic sizing model is employed to design the main parameters of the system in different sizing points (i.e. cold and hot ground, ceiling and cruise conditions). The system parameters are then used to setup the dynamic model. The air cycle technology is employed to provide cold air and the electric dedicated compressors are used to deliver the necessary pneumatic power to the system and to provide cabin pressurization. The main system components such as the dedicated compressors, the cold air unit and the necessary heat exchangers are modeled and described. The models are applied to a turboprop regional aircraft carrying 80 passengers. The results are in line with the expectations and show a greater efficiency of the electrified system compared to the standard one throughout the different mission phases.

I. Nomenclature

ACM	Air Cycle Machine
BLDC	Brushless Direct Current
c_p	specific heat of air at constant pressure $\left[\frac{J}{kg \cdot K}\right]$
C_{max}	maximum heat capacity rate $\left[\frac{W}{s}\right]$
C_{min}	minimum heat capacity rate $\left[\frac{W}{s}\right]$
COND	Condenser
ECS	Environmental Control System
E-ECS	Electric-Environmental Control System
I	air intake
ISA	International Standard Atmosphere
LCD	Liquid Crystal Display
M	electric motor
M_0	Mach number of the air entering the air intake $[-]$

¹ Professor, Department of Mechanical and Aerospace Engineering, AIAA Member.

² Senior researcher, Department of Mechanical and Aerospace Engineering, AIAA Member

³ Researcher, Department of Mechanical and Aerospace Engineering.

\dot{m}_{ECS}	air mass flow provided by the air conditioning system [kg/s]
MIX 1	First mixer
MIX 2	Second mixer
P_c	power of the dedicated compressor [W]
$P_{c,ACM}$	power of the ACM compressor [W]
P_{motor}	power of the electric motor that drive the dedicated compressor [W]
PHE	Primary Heat Exchanger
$\dot{q}_{avionics}$	heat flow due to the avionic system [W]
\dot{q}_{cond}	heat flow due to the fuselage thermal conductivity [W]
$\dot{q}_{display}$	heat flow due to the displays [W]
\dot{q}_{lights}	heat flow due to the lights system [W]
\dot{q}_{met}	heat flow due to the metabolic heat dissipated from occupant [W]
$\dot{q}_{rad\ transp\ sur}$	heat flow due to the solar radiation throughout transparent surfaces [W]
\dot{q}_{tot}	total heat flow throughout the fuselage [W]
RHE	Reheater
SFC	Specific Fuel Consumption
SHE	Secondary Heat Exchanger
T	Turbine
T_1^0	total temperature of the air exiting the air intake [K]
T_2	air temperature of the primary flow entering in the PHE [K]
T_{cab}	desired cabin air temperature [K]
T_{ECS}	temperature of the air leaving the conditioning system [K]
β_c	pressure ratio of the dedicated compressor
$\beta_{c,ACM}$	pressure ratio of the ACM compressor
$\beta_{t,ACM}$	pressure ratio of the ACM turbine
γ	heat capacity ratio of the air [$-$]
ε_{ai}	efficiency of the air intake
$\eta_{is,c}$	isentropic efficiency of the dedicated compressor
$\eta_{is,c,ACM}$	isentropic efficiency of the ACM compressor
$\eta_{is,t,ACM}$	isentropic efficiency of the ACM turbine
η_{mec}	dedicated compressor mechanical efficiency
$\eta_{mec,c}$	mechanical efficiency of the ACM compressor
$\eta_{mec,t}$	mechanical efficiency of the ACM turbine
η_{motor}	electric motor efficiency

II. Introduction

Since last decades one of the most important requirements within the aircraft industry is to reduce the environmental impact and cost of the aircraft product. Different ways are being explored to satisfy these requirements. New technologies that range from laminar aerodynamics, lightweight materials for structure, to propulsion and on-board systems electrification are being investigated. Systems electrification focuses on the electrification of different subsystems that nowadays use other kinds of power sources such as hydraulic and pneumatic power. The main developments are focused on the use of electromechanical and/or electro-hydrostatic actuators to enterally remove the hydraulic system and the electrification of the Environmental Control System (ECS) and Ice Protection System (IPS) to remove or reduce the size of the bleed system [1],[2],[3],[4]. Especially for the ECS, its electrification increases its efficiency by virtually avoiding the dependency with engine speed. The traditional ECS relies on bleed air supplied by the engine compressor. Since the system is sized considering One Engine Inoperative (OEI) condition and engine running at low speed, the system is oversized in normal conditions. Therefore, during the greater part of the flight, the traditional bleed system provides air with temperature and pressure that are excessive for the correct ECS functioning. To avoid that, a heat exchanger and a lamination valve are needed to reduce the air temperature and pressure. In some mission phases this represents an important waste of energy [5],[6],[7],[8]. Hence, with the aim of reducing the fuel consumption and environmental emissions, the ECS, which is the most power demanding aircraft systems, is electrified. In particular, a series of electric compressors replace the bleed system providing compressed air having a pressure and temperature already compatible with the ECS functioning. Different sizing and dynamic models have been developed to estimate the behavior of the conventional ECS, whereas only a few models are focused on the Electric Environmental Control System (E-ECS) [9], [10], [11]. However, those models require a relatively high number of detailed data that cannot be known during the initial design phases. Compared to those models, the one proposed in this paper requires relatively low number of data that can be usually estimated during the first design iterations. Therefore, in this paper a simplified thermodynamic sizing methodology is described focusing on the main

E-ECS components such as the dedicated electric compressors, the primary and secondary heat exchangers, the Cold Air Unit (CAU) and other main components. A dynamic model is then setup using the results of the sizing model to characterize the different components. In this way, it is possible to provide the desirable design continuity useful during the first phases of aircraft design. Then the models are applied to a new turboprop regional aircraft carrying 80 passengers to evaluate the feasibility, scalability, and the performance of the E-ECS technology.

III. Simplified thermodynamic sizing model for Electric-Environmental Control System

The model already developed [12] is divided into two main parts that are: the heat loads calculation and the E-ECS sizing. The heat loads module estimates the heat loads due to the passengers and the crew members \dot{q}_{met} , the avionics $\dot{q}_{avionics}$, the internal lights \dot{q}_{lights} and the flight entertainment system $\dot{q}_{display}$ starting from some aircraft and mission information. Additionally, the heat loads due to the external environment are also taken into account. In particular, two main contributions are considered: the heat load due to the fuselage thermal conductivity \dot{q}_{cond} and the heat load generated by the solar radiation coming through the transparent surfaces (i.e., cabin windows and windshields) $\dot{q}_{rad\ transp\ sur}$.

$$\dot{q}_{tot} = \dot{q}_{met} + \dot{q}_{avionics} + \dot{q}_{display} + \dot{q}_{lights} + \dot{q}_{cond} + \dot{q}_{rad\ transp\ sur} \quad [W] \quad (1)$$

The metabolic heat load \dot{q}_{met} is calculated considering the standard [13] heat load per person differently for a passenger and a crew member (i.e., 70 and 130W). The heat loads due to electric and electronic equipment are calculated starting from their electric consumption multiplied by a ratio between the power absorbed and the thermal power emitted. Those heat flows are strongly dependent on the technologies used. Considering the test case selected, the latest technologies for lights and displays are selected. They are led technology for internal lights and LCD for the displays used for the flight entertainment system. All kind of internal lights are here considered, the aisle lights, the floor lights and the reading lights provided to passengers. The thermal load due to fuselage conduction \dot{q}_{cond} is modeled using an equivalent electric circuit. Three main fuselage layers are considered: the plastic/composite internal layer, the isolating microlite layer and the external one constituted by aluminum or composite material. For \dot{q}_{cond} estimation is important to correctly calculate the internal and external wall temperatures as defined in [13]. However, during flight condition, the model assumed that the external wall temperature coincided with the recovery temperature [14]. Finally, the heat flow due to solar radiation from windows and windshields $\dot{q}_{rad\ transp\ sur}$ is calculated considering the total transparent surface divided by a coefficient of 2 to take into account that having a sole radiation source (i.e. the sun) the radiation can penetrate from, at maximum, the half of the windows at the same time.

In Table I, the main inputs for the heat loads estimation model are listed.

Table I Sizing model input

Input	Value	Unit
Number of passengers	80	
Number of crew members	4	
Passenger thermal power	70	[W]
Crew thermal power	130	[W]
Avionics thermal power	1000	[W]
Displays thermal power	8.4	[W]
Number of displays (for in-flight entertainment)	80	
Internal skin thickness	0.005	[m]
Microlite layer thickness	0.055	[m]
External skin thickness	0.001	[m]
Transparent surface (windows + windscreen)	5.1	[m ²]
Cruise Mach	0.4	

Having calculated the heat flow to be balancing during the aircraft operation, the second part of the E-ECS sizing module can be applied. As showed in Fig. 1, the E-ECS is composed by an air intake that collect and slightly compress external air to be sent to the dedicated centrifugal compressors and to the precooler. The centrifugal compressors are driven by electric motors connected to the high voltage electric bus of the Electric Power Generation and Distribution System (EPGDS). The dedicated compressors provide compressed and hot air that is used for cabin pressurization and to heat it when needed. Part of this compressed air is cooled by the precooler to be sent to the Air Cycle Machine (ACM). The precooler is an air-to-air heat exchanger that uses the external air to cool the compressed air coming from the dedicated compressors. The ACM provides cold air when the cabin needs to be cooled. Anyway, the mixing unit combines hot and cold air to control cabin temperature. Part of the cabin air is constantly evacuated out board after having cooled the avionic system (or part of it). Another E-ECS lane having the same components can be envisaged to fulfill the safety requirements.

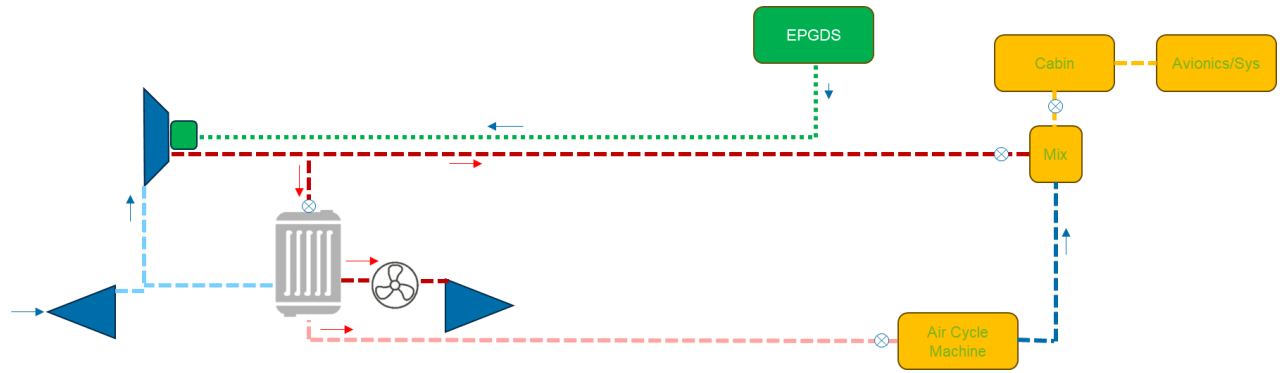


Fig. 1 E-ECS schematic

Starting from total fuselage heat load \dot{q}_{tot} , it is possible to size the E-ECS calculating the air flow necessary to balancing cabin heat load. The air mass flow \dot{m}_{ECS} is defined as:

$$\dot{m}_{ECS} = \frac{\dot{q}_{tot}}{c_p(T_{ECS} - T_{cab})} \quad [kg/s] \quad (2)$$

Where the c_p is the air specific heat, T_{ECS} the air temperature measured at E-ECS outlet and the T_{cab} is the desired temperature of the air in the cabin. Therefore, the sizing module performs a thermodynamic design of all main system components to calculate the total power required by the E-ECS that is the power needed by the dedicated compressors. Each component is modeled to calculate the inlet and outlet air temperature, pressure, and mass flow. The air intake is assumed having quasi-ideal performance supposing that its capture section is coincident to its entrance section neglecting the effect of the fuselage. Moreover, assuming an almost static outflow, the output pressure and temperature match with those calculated for the stagnation conditions. An efficiency close to 0.9 is considered during flight. Focusing on the motor driven compressors, it is assumed that they are of the centrifugal type considering their compactness and high compression ratio. The power needed by the dedicated compressors is estimated using the following:

$$P_c = \frac{\dot{m}_{ECS} \cdot c_p \cdot T_1^0}{\eta_{is,c}} \left[\beta_c^{\frac{\gamma-1}{\gamma}} - 1 \right] \quad [W] \quad (3)$$

Where the T_1^0 is the total temperature of the air exiting the air intake, $\eta_{is,c}$ is the isentropic efficiency of the dedicated compressor, and β_c is the pressure ratio of the dedicated compressor. The main sizing points are:

- The on-ground cooling condition during hot day due to the high airflow at medium pressure required to obtain enough cooled air from the ACM
- The heating condition during flight due to the relative high compression needed to pressurize the cabin

The sizing module uses a generic centrifugal compressor map to estimate the compression efficiency $\eta_{is,c}$ by varying β_c and \dot{m}_{ECS} (see Fig. 2)

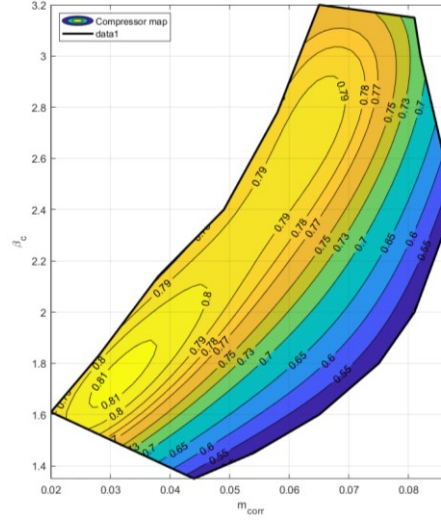


Fig. 2 Centrifugal compressor map

To fully calculate the power required by the ECS system, the electric power of the motors which drive the compressors has to be estimated. The following formula is here considered:

$$P_{motor} = \frac{P_c}{\eta_{motor} \cdot \eta_{mec}} \quad [W] \quad (4)$$

Where: η_{mec} is the mechanical efficiency of the compressor and η_{motor} is the efficiency of the electric motor. The last unknown to calculate the \dot{m}_{ECS} and then the P_{motor} is the T_{ECS} . The outlet temperature from E-ECS can be calculated only modelling the ACM unit. The ACM selected is a two-wheels bootstrap cycle composed by a compressor, a turbine, two heat exchangers (primary and secondary), a condenser, and a mixer unit.

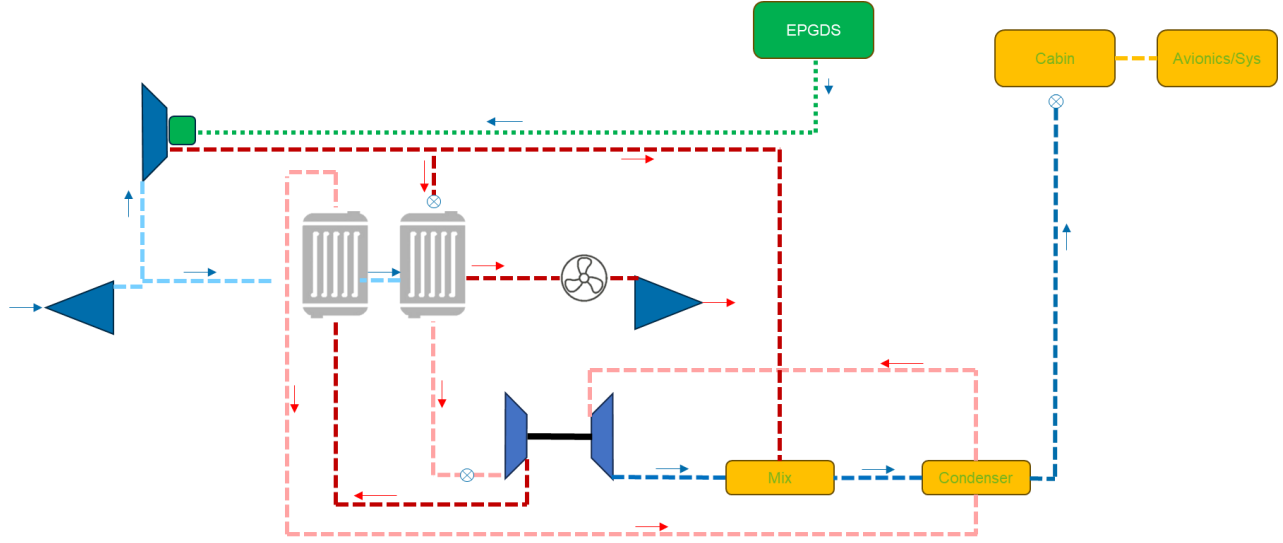


Fig. 3 E-ECS schematic with ACM components

Following the airflow of the primary flow (i.e. part of the airflow provided by the dedicated compressors that flows throughout the ACM) the first element is the primary heat exchanger. It is an air-to-air heat exchanger that is used to cool the hot and compressed air coming from the dedicated compressors. The cooling effect is provided by the external air flowing in the secondary flow (i.e. the airflow of external air that flows through the air intake, the two heat exchangers, the fan, and then, it is sent overboard). The secondary flow is set in motion by the dynamic air when the aircraft is in flight or by a dedicated electric fan during ground operations. To calculate the temperature of the primary and secondary outlet flows the followings equations are used:

$$\dot{q} = \epsilon \cdot C_{min} \cdot |T_{1,in} - T_{2,in}| \quad [W] \quad (5)$$

$$C_{min} = \min \left\{ (\dot{m} \cdot c_p)_1, (\dot{m} \cdot c_p)_2 \right\} \quad [W/s] \quad (6)$$

Where \dot{q} : is the thermal power [W],

ϵ : effectiveness of the heat exchanger;

C_{min} : minimum heat capacity rate $\left[\frac{kg}{s} \cdot \frac{J}{kg \cdot K} \right]$;

$T_{1,in}$: inlet temperature of the primary flow [K];

$T_{2,in}$: inlet temperature of the secondary flow [K].

The effectiveness of the heat exchanger is estimated using the Number of Transfer Unit (NTU) model [16] and the a typical effectiveness versus NTU diagram provided by [17]. The outlet temperature of the primary and secondary flows can be calculated with the following:

$$T_{2,out} = T_{2,in} \mp \frac{\dot{q}}{(\dot{m} \cdot c_p)_2} \quad [K] \quad (7)$$

The second element encountered by the primary flow is the ACM compressor. It is needed to compress the air that after a cooling in the secondary heat exchanger and an expansion in ACM turbine become sufficiently cold to be used to cool the cabin during the worst hot day conditions. The flow temperature at the ACM compressor outlet and the compressor power $P_{c,ACM}$ are calculated using the followings:

$$T_{out}^0 = T_{in}^0 \left[1 + \frac{1}{\eta_{is,c}} \left(\beta_c^{\frac{\gamma-1}{\gamma}} - 1 \right) \right] \quad [K] \quad (8)$$

$$P_{c,ACM} = \dot{m} \cdot c_p (T_{out}^0 - T_{in}^0) \quad [W] \quad (9)$$

Where $\eta_{is,c}$ is the isentropic compression efficiency and β_c is the compressor pressure ratio. As mentioned before, the next step is to cool the compressed air using the secondary heat exchanger. The outlet temperature of the primary and secondary flows is calculated using the equations 5, 6 and 7. To obtain the cold air needed during cooling phases the air exiting the secondary heat exchanger is expanded in the ACM turbine unit. However, before the expansion, the airflow should be dried to avoid water or ice formation in the turbine unit reducing possible damages. Therefore, the condenser unit is needed. It is a type of heat exchanger that uses the cold air provided by the ACM to condensate the water. By means of a water separator, the water is then eliminated. The condenser has been modeled as a heat exchanger calculating the total heat exchanged as the sum of the sensible and latent heat. More details can be found in [12].

At this point, the airflow can be expanded in the ACM turbine. To calculate the airflow outlet temperature and the power produced by the turbine $P_{t,ACM}$ the following are defined:

$$T_{out}^0 = T_{in}^0 \left[1 - \eta_{is,t} \left(1 - \frac{1}{\beta_t^{\frac{\gamma-1}{\gamma}}} \right) \right] \quad [K] \quad (10)$$

$$P_{t,ACM} = \dot{m} \cdot c_p (T_{in}^0 - T_{out}^0) \quad [W] \quad (11)$$

Where $\eta_{is,t}$ is the efficiency of the isentropic expansion and the β_t is the expansion pressure ratio. The ACM compressor and the ACM turbine are connected on the same axle, it means that the power needed to compress the airflow entering the compressor is provided by the expansion in the turbine. Therefore, the following condition must be verified:

$$P_{t,ACM} \cdot \eta_{mec,t} = \frac{P_{c,ACM}}{\eta_{mec,c}} \quad [W] \quad (12)$$

Where the $\eta_{mec,t}$ and $\eta_{mec,c}$ are the mechanical efficiency of, respectively, the ACM turbine and compressor. Finally, the airflow reaches the mixing unit which mixes the cold air coming from the ACM with the hot air produced by the dedicated compressors. In this way a large range of temperatures can be reached to fulfill the cabin environmental control requirements. The outlet flow psychometric characteristics is calculated balancing the mass flow rate and the enthalpy of the inlet flows.

IV. E-ECS dynamic model

Starting from the results of the sizing model a dynamic model of the E-ECS has been developed using Simcenter AMESim software. The main difference between the two models is that the first one is able to estimate the static behaviors of the main variables performing a first thermodynamic sizing, the second one provides the dynamic of the system and its components. In Fig. 4, the E-ECS dynamic model is depicted. On the left side of the schematic, the dedicated electric compressors are defined as a two stages centrifugal compressor driven by a BrushLess Direct Current (BLDC) motor. The two stages are connected to the same shaft. The air intake is simulated as an air source having a total pressure, total temperature and airflow in accordance with the analytical model for the different design conditions. On the right side, the primary and secondary heat exchangers, the ACM, the condenser, the fan and the mixing unit are defined. All the components and their parameters have been defined in agreement with the analytical model. To keep low the complexity of the model, the heat exchangers efficiency is an input and derived from the sizing model. More detailed models of heat exchangers are available, but the level of the required inputs would have required real product data going beyond the purpose of the model. The compressors are modeled through a lookup table consisting of the operating points defined in the compressor map already used in the sizing model (Fig. 2). For the ACM compressor and turbine, a constant efficiency is considered since the ACM speed is almost constant when not by-passed.

In line with real ECS some valves have been added to manage the air conditioning pack. In particular, at the bottom of the schematic, it is possible to notice a pack valve, a by-pass valve and an ACM valve. The pack valve manages the airflow entering the whole pack and its pressure. The by-pass and ACM valves work together to allow or not the airflow entering on the ACM. In general, when the ECS have to cool the cabin, all the airflow passes through the ACM. When the ECS must warm the cabin, the ACM valve is almost closed, and the by-pass valve is opened to allow the hot air to go into the cabin mixer.

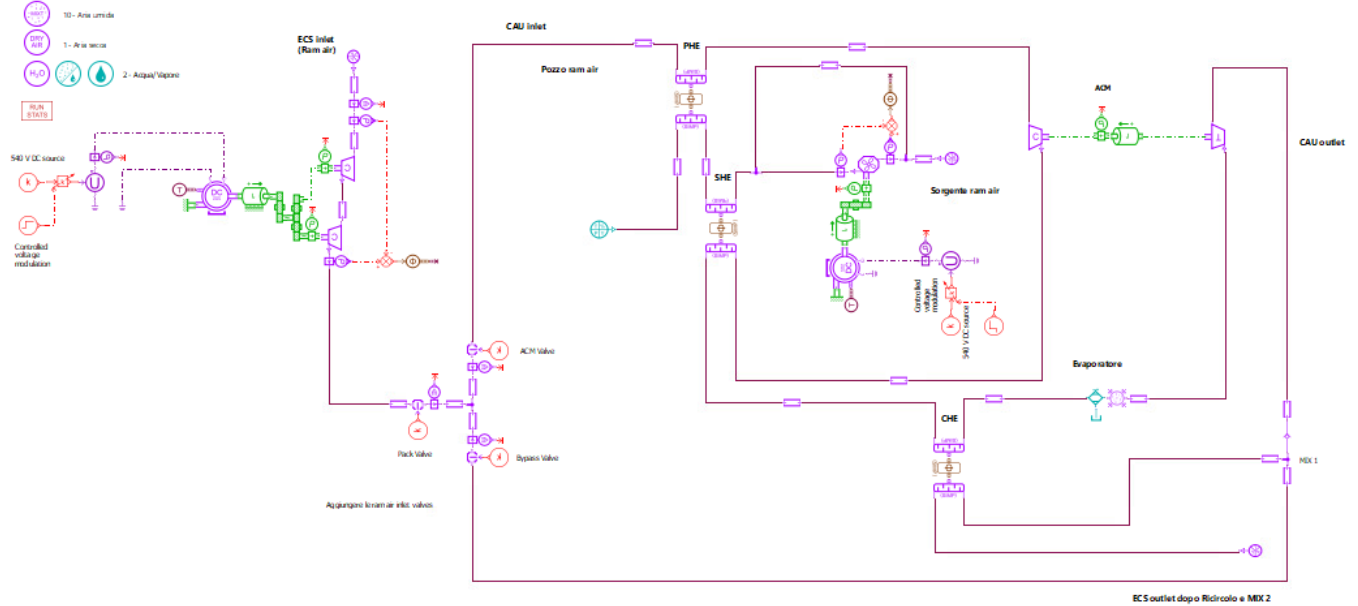


Fig. 4 E-ECS Dynamic model

The parameters of the dynamic model are in line with the input of the sizing model. The main parameters regarding the aircraft are already provided in Table I. In Table II the main parameters for the ECS components are listed. They

represent the detailed E-ECS input regarding the main components such as the compressors, the turbine and the electric motors.

Table II Main parameters for E-ECS components

Detailed input	Unit of measure	hot day ISA+25 (ground)	cold day ISA-35 (ground)	cold day ISA - 20 (climb)	hot day ISA+20 (ceiling)
Isentropic efficiency of the ACM compressor	-	0.77	0.7	0.75	0.75
Isentropic efficiency of the ACM turbine	-	0.8	0.7	0.75	0.75
Mechanical efficiency of the ACM	-	0.98	0.98	0.98	0.98
Fan Efficiency	-	0.68	0.68	0.68	0.68
Mechanical efficiency of the fan	-	0.95	0.95	0.95	0.95
Electric Motor Fan efficiency	-	0.93	0.93	0.93	0.93
PHX efficiency	-	0.87	0.87	0.87	0.87
SHX efficiency	-	0.87	0.87	0.87	0.87
CHX efficiency	-	0.59	0.59	0.59	0.59
Pressure losses of the ram air	Pa	6000	6000	6000	6000
Pressure losses of the recirculation air	Pa	5000	5000	5000	5000
Cabin air temperature	°C	27	21	21	25

The model is defined in order to simulate the following operating conditions: hot ground, cold ground, cold ceiling, and standard ISA cruise as defined in Table III. All of them are considered as possible sizing points for the E-ECS. The hot ground condition is the most demanding in terms of cold air flow due to the highest number of passengers and the maximum external temperature and solar radiation. Conversely, the condition that requires the maximum hot air flow is not easily identified. However, they should be the cold ground or the cold ceiling. Moreover, the cold ceiling is the most demanding condition for aircraft pressurization. The standard ISA cruise provides the nominal consumption of the system. In the dynamic model, the whole aircraft mission is considered with ambient parameters varying continuously as depicted in Fig. 5.

Table III Operating Conditions

Operating conditions	External temperature [K]	External pressure [bar]	Flight Mach	Altitude [m]	Passengers number	Specific humidity	Relative humidity %
Hot ground	314.15	1.013	0	0	80	0.0172	35
Cold ground	253.15	1.013	0	0	0	0.0002	28
Cold ceiling	214.15	0.377	0.4	7600	0	0	50
Standard ISA cruise	254.45	0.527	0.4	5200	70	0.0007	40

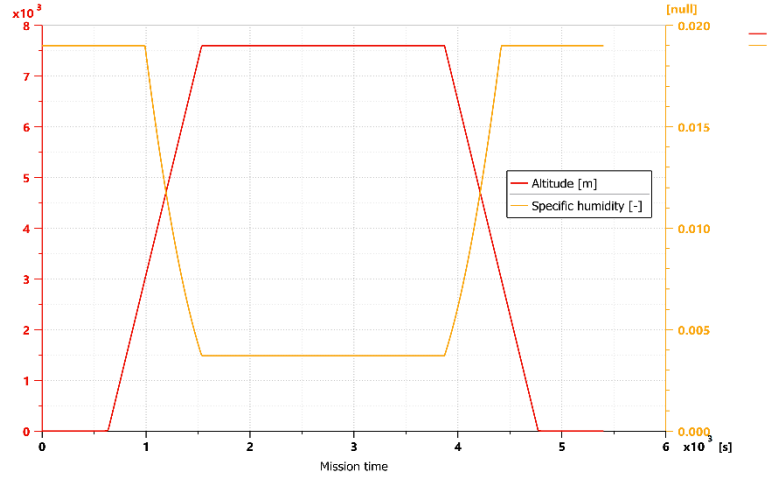


Fig. 5 Ambient specific humidity within the mission profile

V. Results of the analysis

As described in the previous chapters, the model simulates the E-ECS behaviors for an 80 passengers aircraft for the main four sizing conditions. The results regarding the pneumatic power generation are listed in Table IV. The main parameters of the external air are defined together with the outlet flow of the 1st and 2nd stage of the dedicated compressor. The starting pressure and temperature values of the external air are in line with the defined sizing conditions. It is worth noting that the hot ground and cold ceiling conditions are the sizing points for the dedicated compressor. In the first condition, the high pressure and airflow values are needed to supply the ACM to generate cold air. In the second condition, those values are needed to pressurize and warm the cabin almost by-passing the ACM. An efficiency of 0.92 is estimated for the electric system generator to calculate the engine power offtakes.

Table IV E-ECS pneumatic power generation

Pneumatic power generation		Hot ground	Cold ground	Cold ceiling	Std ISA cruise
external conditions	T [K]	314	253	221	262.65
	p [bar]	1.013	1.013	0.41	0.573
	x [-]	0.0172	0.0002	0	0.0007
	phi [%]	35	28	0	40
	dm [g/s]	434.7	210.82	620.99	216
Dedicated compressor 1st stage	T [K]	376.99	278.8	265.46	321.83
	p [bar]	1.728	1.379	0.669	1.042
	beta c	1.715	1.363	1.715	1.825
	omega [rpm]	25829	16452	22023	25277
Dedicated compressor 2nd stage	T [K]	440.91	304.52	303.15	382.94
	p [bar]	2.751	1.83	1.199	1.741
	beta c	1.592	1.327	1.575	1.67
	omega [rpm]	25829	16452	22023	25277
Dedicated compressor electrical power	P[kW]	69.08	13.01	69.73	26.00

Dedicated compressor mechanical power to engine gearbox shaft	P[kW]	75.09	14.14	75.79	28.26
---	-------	-------	-------	-------	-------

In Table V, the results of each component pertaining to the primary flow are listed. In cold ground and cold ceiling conditions, the ACM is bypassed therefore no data are listed for these two conditions. In the other sizing points, the performance of the ACM and its components are almost in line with the results of the sizing model. Comparing the airflows in Table IV and Table V, it is worth noting that all the airflow passes through the ACM in hot ground condition whereas in standard ISA cruise only the half of the airflow is used by the ACM. This is mainly due to the thermal load. In the first case, the air conditioning pack have to produce cold air. In the second case, the cold air has to be mixed with bypassed air to reach the thermal balancing in the cabin at comfortable temperature.

Table V Results of the E-ECS primary flow

		Hot ground	Cold ground	Cold ceiling	Std ISA cruise
PHX inlet	T [K]	440.91	-	-	382.94
	p [bar]	2.751	-	-	1.741
	x [-]	0.0172	-	-	0.0007
	dm [g/s]	434.7	-	-	102.35
PHX outlet	T [K]	351.73	-	-	341.5
	p [bar]	2.674	-	-	1.734
ACM compressor out	T [K]	398.8	-	-	349.7
	p [bar]	3.876	-	-	1.858
	beta_c	1.449	-	-	1.072
	omega [rpm]	27915	-	-	7930
SHX out	T [K]	325.19	-	-	276.94
	p [bar]	3.845	-	-	1.856
Condenser HP side	T [K]	300.27	-	-	292.87
	p [bar]	3.833	-	-	1.855
Evaporator	dm air out [g/s]	429.55	-	-	102.28
	T [K]	300.27	-	-	292.87
	p [bar]	3.258	-	-	1.654
	phi in [%]	12.56	-	-	9.08
	phi out [%]	0	-	-	0
ACM Turbine	T [K]	238.72	-	-	272.83
	p [bar]	1.317	-	-	1.254
	beta_t	2.47	-	-	1.319
Condenser LP side	T [K]	270	-	-	295.45
	p [bar]	1.186	-	-	1.062
Mixer	T [K]	238.72	-	-	330.89
	p [bar]	1.201	-	-	1.15
Outlet	T [K]	269.32	-	-	295.45
	p [bar]	1.453	-	-	1.062
	x [-]	0	-	-	0.0005

In Fig. 6 and Fig. 7 the temperatures and the pressures of the primary flow passing through the main ECS components are depicted. In particular, only hot-ground and the standard ISA cruise conditions are there reported since during only these two sizing conditions the ACM is not bypassed. In hot ground condition the outlet temperature is 269K (-4.15°C) whereas in Std ISA condition is 295.45K (22.4°C). Fig. 7 better explains the difference between the two conditions. To cool the cabin, in hot ground, the ACM has to be supplied with high pressure air, this increases the ACM speed increasing further the air pressure through the ACM compressor. The heat extraction from radiators and the expansion in the ACM turbine generates the needed cold air. In cruise conditions, the ACM is partially active, and the supply pressure is quite low even considering the lower external pressure.

The temperatures and pressures estimated for the electric pneumatic power generation section of the E-ECS are showed in Fig. 8 and Fig. 9. In this case all the system sizing conditions are reported.

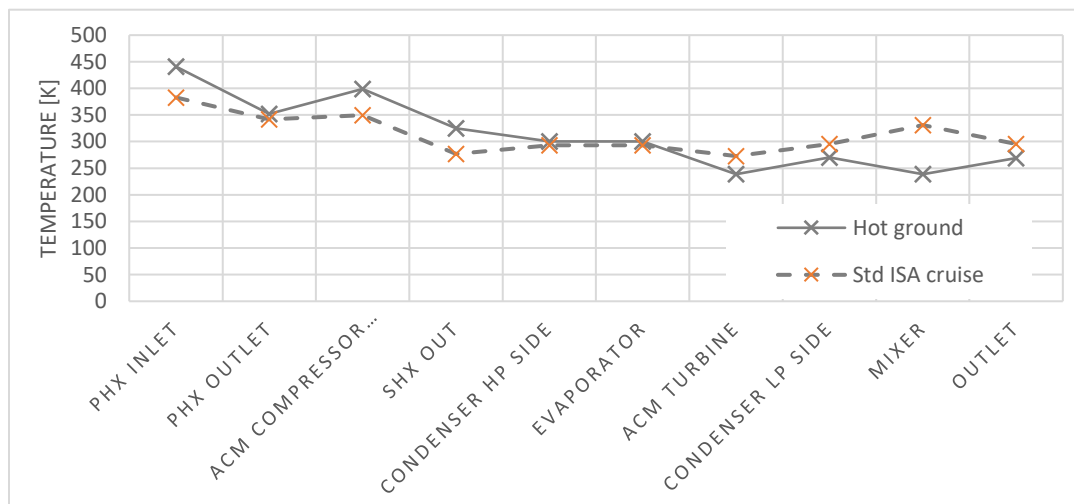


Fig. 6 Temperature for each EECS component

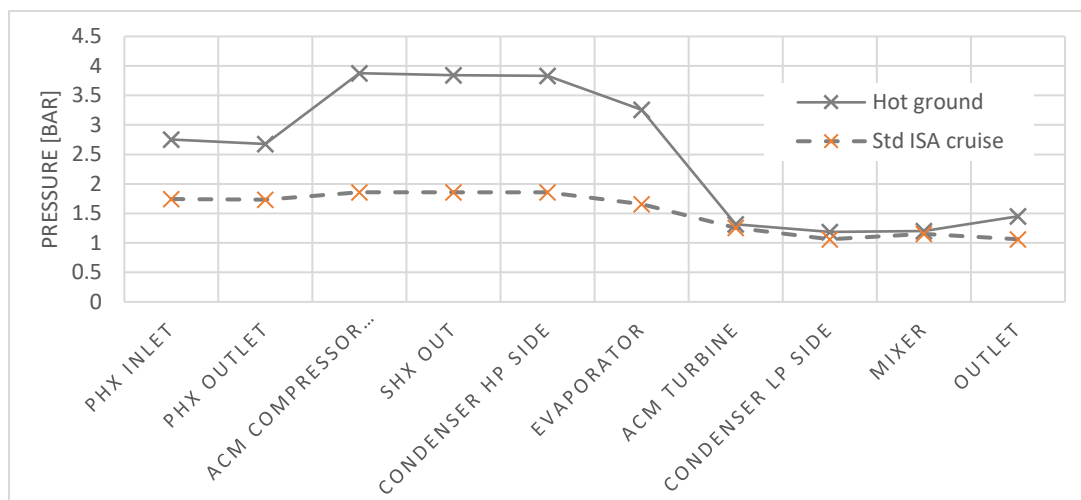


Fig. 7 Pressure for each EECS component

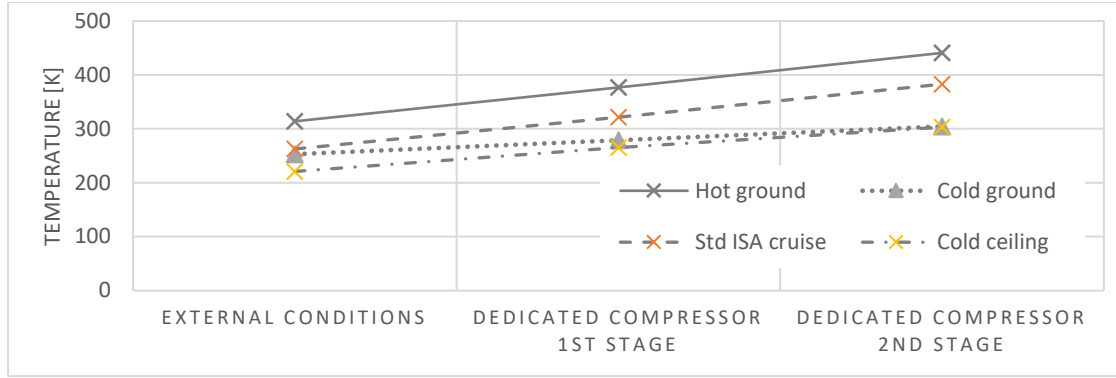


Fig. 8 Electric pneumatic power generation, temperature for each element

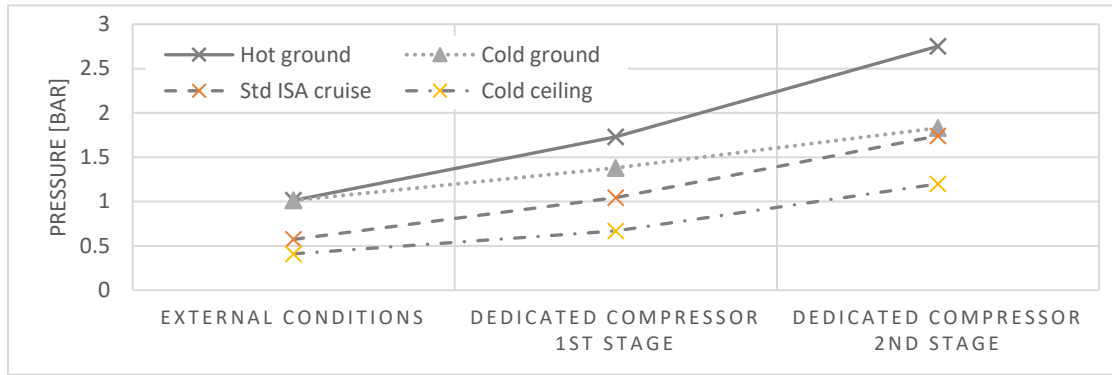


Fig. 9 Electric pneumatic power generation, pressure for each element

The dynamic model has been employed to verify the dynamic performance of the E-ECS components during heating and cooling phases. In particular, two missions are implemented both having a mission profile as depicted in Fig. 5 where the take-off, climb, cruise, descent and landing phases are defined. The first mission is set up to reach the cold ground and cold ceiling sizing points. The second mission reaches the hot ground and standard ISA cruise sizing points. On the left of Fig. 10, the mass flow rate calculated at the E-ECS inlet and at the by-pass duct are showed during the first mission. The mass flow rates coincide to the same values because the E-ECS is always in heating condition and the ACM is completely bypassed. The mass flow rate increases with aircraft altitude reaching the maximum value in cruise (cold ceiling conditions). This is due to the external air conditions where a higher compression and temperature is required to compensate the cabin pressure and balancing the thermal load. It is also important to consider that the compression ratio and the mass flow of a centrifugal compressor are coupled together. On the right side of Fig. 10, the mass flow rate calculated at the E-ECS inlet, at the ACM inlet and at the by-pass duct are depicted for the second mission. Here, the total part of the primary flow passes through the ACM at the beginning of the mission. However, to maintain the right cabin temperature during the climb and cruise phases a portion of the flow is bypassed and mixed before entering the cabin. In Fig. 11, the ACM shaft speed, power and pressure ratio is depicted for the second mission when the ACM is actually employed. It is possible to note that the ACM is fully active in hot ground conditions when it is needed to provide cold air. After this phase the ACM is increasingly bypassed reducing its pressure ratio and shaft speed. It is possible to see a small overshooting when the mission phase change from taxi/takeoff to climb. Initially, the dedicated compressor tries to compensate the decrease of supplied pressure increasing the shaft speed. However, this produces a colder air than required and the bypass valve is operated to reduce the ACM shaft speed and to increase the outlet air temperature.

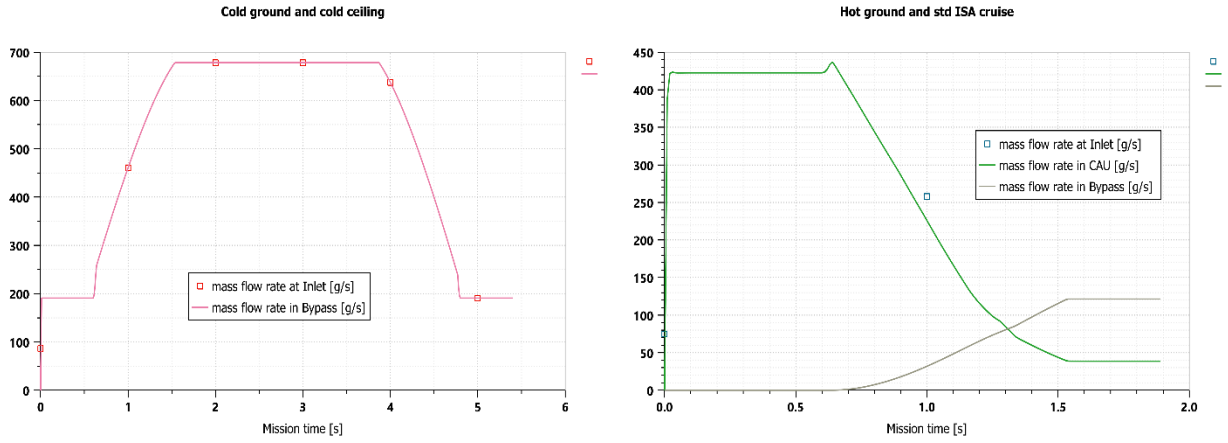


Fig. 10 Mass flow rate at the E-ECS inlet and at the by-pass duct during aircraft flight in heating conditions (left). Mass flow rate at the E-ECS inlet, at the ACM inlet and at the by-pass duct during aircraft take-off, climb and cruise in cooling conditions (right).

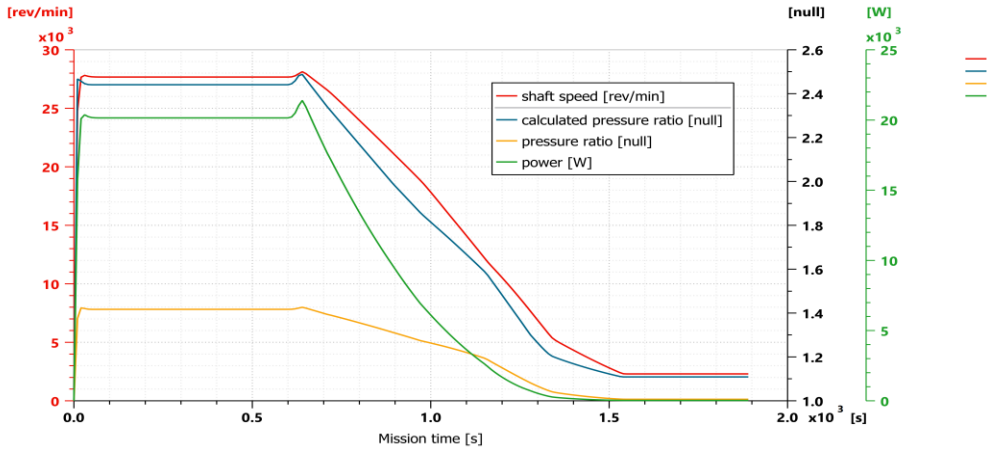


Fig. 11 ACM shaft speed, power and pressure ratio during aircraft take-off, climb and cruise in cooling conditions

Fig. 12 shows the dedicated compressor shaft speed and pressure ratio for each of its two stages. On the left side of the figure, the dedicated compressor parameters are depicted for the first mission. Here, the E-ECS has to warm the cabin air both in ground and in flight. As the compressor parameters show, it is fully active in flight (cold cruise conditions) where the cabin has to be pressurized and the warming requirement reach the maximum due to the colder external air and the thermal convection activated by aircraft speed. In the second mission, depicted on the right side of Fig. 12, the parameters of the dedicated compressor are more stable. The system is required to work at its maximum power since in hot ground conditions both high pressure and air flow are needed to cool the cabin, in hot cruise conditions they are required essentially to provide pressurization but also a small quantity of cold air to be mixed with the bypassed one to provide a not too hot air to the cabin. It is clear by Fig. 12 that the sizing points of the dedicated compressor are reached in the second mission.

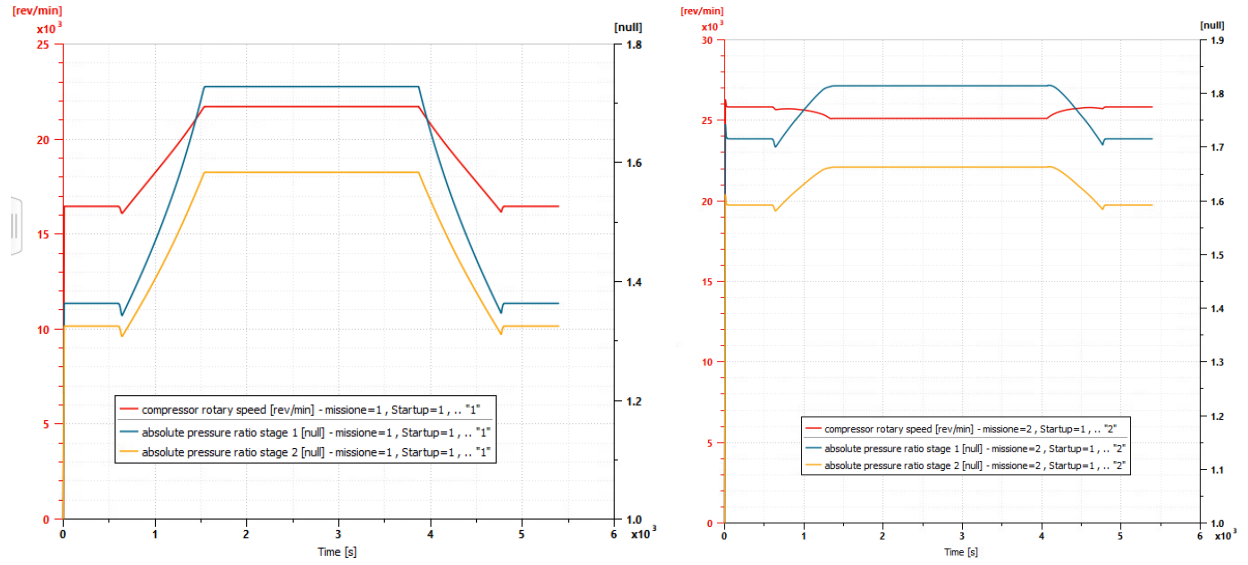


Fig. 12 Dedicated compressor speed and stage pressure ratios during aircraft flight in heating conditions (left). Dedicated compressor speed and stage pressure ratios during aircraft take-off, climb and cruise in cooling conditions (right).

Finally, a comparison with the traditional alternative (i.e. ECS with bleed system) is here provided. In Table VI, the parameters of a possible bleeding system are provided. The bleed system is treated as a mechanical compressor having two main sizing points: hot ground for the pressure ratio, and cold ceiling for the air flow. These are conservative assumptions since the engine compressors are not primarily sized to satisfy the bleed system requirements, but the engine power or thrust. Therefore, in a real case, the bleed system is often able to supply more pressure and air flow than required reducing its efficiency. Since the compression ratio is dependent to the engine speed. In some case, the bleed system produces more pressure than required. However, when the ECS has to warm the cabin, the more compressed and hotter air reduces the air flow requirement as can be seen comparing Table VI with Table IV. In Table VII the E-ECS and the traditional ECS are compared. As could be predicted, in hot ground sizing conditions the traditional system is more efficient since it does not need to furtherly convert the mechanical power to the electrical power to supply the dedicated compressor. In all the other conditions the E-ECS is more efficient since the compressor speed can be managed separately respect to the engine speed.

Table VI Possible bleed system parameters in the different sizing conditions

Conditions	Hot ground	Cold ground	Cold ceiling	Std ISA cruise
Pressure [bar]	2.751	2.751	1.937	2.330
Temperature [K]	440.91	440.91	366.15	454.15
Air flow [g/s]	434.7	145.6	514.1	182.1
Power [kW]	69.08	28.64	78.11	36.51

Table VII Comparison between the E-ECS and the traditional ECS

Conditions	Hot ground	Cold ground	Cold ceiling	Std. ISA cruise
E-ECS power [kW]	75.09	14.14	75.79	28.26
Traditional ECS power [kW]	69.08	28.64	78.11	36.51
E-ECS power (Traditional ECS power as reference) %	8.7	-50.6	-3.0	-22.6

VI. Conclusion

The sizing and dynamic models described in this paper provide results in line with the expectations increasing the details of the E-ECS operation. The implemented models are quite flexible and can be applied to different aircraft categories and dimensions. The sizing model requires a small amount of data that can be easily known during the first aircraft design iterations. The results of that model are then used as input for the more detailed dynamic model to obtain a good continuity of the E-ECS design during the initial aircraft design phases. The results show that the E-ECS is more efficient compared to the traditional ECS for most of the sizing points and during the standard cruise. In that case, the E-ECS requires about 22% less power. This is a important result considering that the ECS is the most power demanding system and that the cruise phase is usually the longest part of the flight. The E-ECS increases the overall system efficiency by providing the correct amount of pneumatic power whereas the traditional bleed system is almost always oversized. Only during the hot ground sizing conditions, the traditional ECS performs better reducing the number of power conversions.

It is worth noting that the comparison is carried out in the sizing conditions except for cruise, and it is assumed that the engine compressor is designed to exactly satisfy the ECS requirements. These should be considered as conservative assumptions to prove the feasibility of the E-ECS. In a real case, the bleed system could be oversized especially in turboprop engines where there are, usually, a limited number of centrifugal compressor stages. Moreover, the advantage of the E-ECS is to perform better during nominal conditions more than the sizing one. In those case the E-ECS is able to save power due to its flexibility in producing pneumatic power. Moreover, the traditional ECS need pneumatic power whereas the E-ECS mechanical one. The effect on engine SFC of extracting the same quantity of power from the bleed system or from the engine shaft is not the same as bleeding compressed air from engine compressor is more detrimental. Therefore, the power saving obtained in the present analysis should be considered as the minimum saving provided by E-ECS.

Further studies will include a comparison in nominal conditions.

Acknowledgment

This project has received funding from the Clean Aviation Joint Undertaking under the Grant Agreement HERA (Hybrid-Electric Regional Architecture) n° 101102007. The granting authority receives support from the European Union's Horizon Europe research and innovation programme and the Clean Aviation Joint Undertaking members other than the Union.



Disclaimer

Views and opinions expressed are however those of the author(s) only and do not necessarily reflect those of the European Union or Clean Aviation Joint Undertaking. Neither the European Union nor the granting authority can be held responsible for them.

References

- [1] M. J. Cronin, "All-Electric vs Conventional Aircraft: The Production/Operational Aspects," *Journal of Aircraft*, vol. 20, no. 6, pp. 481-486, 1983.
- [2] I. Moir and A. Seabridge, *Aircraft Systems: Mechanical, electrical, and avionics subsystems integration*, Third ed., England: John Wiley & Sons, 2011.
- [3] L. Faleiro, J. Herzog, B. Schievelbusch and T. & Seung, "Integrated equipment systems for a more electric aircraft-hydraulics and pneumatics," in *Proceedings of 24th International Congress of the Aeronautical Sciences*, 2004.
- [4] R. I. Jones, "The more electric aircraft—assessing the benefits," *Proceedings of the Institution of Mechanical Engineers, Part G: Journal of Aerospace Engineering*, vol. 216, no. 5, pp. 259-269, 2002.
- [5] M. Fioriti, L. Boggero, S. Corpino, P. S. Prakasha, P. D. Ciampa and B. Nagel, "The Effect of Sub-systems Design Parameters on Preliminary Aircraft Design in a Multidisciplinary Design Environment," *Transportation Research Procedia*, vol. 29, pp. 135-145, 2018.
- [6] J. Kurzke, "Gas turbine cycle design methodology: a comparison of parameter variation with numerical optimization," *Journal of engineering for gas turbines and power*, vol. 121, no. 1, pp. 6-11, 1999.
- [7] L. Lupelli and T. Geis, A study on the integration of the IP Power Offtake system within the Trent 1000 turbofan engine. Master Thesis., 2012.
- [8] M. Sinnet, "787 No-Bleed Systems: Saving Fuel and Enhancing Operational Efficiencies," *Aero Quarterly QTR_04 | 07*, pp. 06-11, 2007.
- [9] J. Vargas and A. Bejan, "Thermodynamic optimization of finned crossflow heat exchangers for aircraft environmental control systems," *International Journal of Heat and Fluid Flow*, vol. 22, no. 6, pp. 657-665, 2001.
- [10] T. Planès, S. Delbecq, V. Pommier-Budinger and E. Bénard, "Modeling and Design Optimization of an Electric Environmental Control System for Commercial Passenger Aircraft," *Aerospace*, vol. 10, no. 3, p. 260, 2023.
- [11] L. Patricelli, "Innovative solutions for the thermal control of aeronautic vehicles," Master thesis, 2013.
- [12] M. Fioriti, F. Di Fede, A Design Model for Electric Environmental Control System in Aircraft Conceptual and Preliminary Design. INTERNATIONAL REVIEW OF AEROSPACE ENGINEERING, 2023.
- [13] ASHRAE, "Aircraft," in *Heating, ventilating, and air conditioning: analysis and design*, American Society of Heating, Refrigerating and Air-Conditioning Engineers, Inc., 2015.
- [14] D. W. Green and R. H. Perry, *Perry's chemical engineers' handbook*, vol. 2, McGraw-Hill, 2008, pp. 2-155.
- [15] SAE-AIR-1168/3, "Aerothermodynamic Systems Engineering and Design," SAE aerospace, 2011.
- [16] F. P. Incropera and D. P. DeWitt, *Fundamentals of Heat and Mass Transfer*, 3rd ed., New York: Wiley, 1990, pp. 658-660.
- [17] SAE-AIR-1168/6, "Characteristics of Equipment Components, Equipment Cooling System Design, and Temperature Control System Design," SAE International, 2004.
- [18] Liebherr-Aerospace, "A319/A320/A321 Environmental Control System - Familiarization Training," Liebherr-Aerospace, 2004.
- [19] M. A. Dornheim, "Electric cabin," *Aviation week and space technology*, pp. 47-49, 28 March 2005.